DOI: 10.1002/chem.200902991

The Effect of the Equatorial Environment on Oxo-Group Silylation of the Uranyl Dication: A Computational Study

Ahmed Yahia,[a, b] Polly L. Arnold,[c] Jason B. Love,[c] and Laurent Maron*[a]

Abstract: A theoretical investigation of the reductive oxo-group silylation reaction of the uranyl dication held in a Pacman macrocylic environment has been carried out. The effect of the modeling of the Pacman ligand on the reaction profiles is found to be important, with the dipotassiation of a single oxo group identified as a key component in promoting the reaction between the Si–X and uranium–oxo bonds. This reductive silylation reaction is also proposed to occur in an aqueous environment but was found not to operate on bare ions; in this latter case, substitution of a ligand in the equatorial plane was the most likely reaction. These results demonstrate the importance of the presence but not the identity of the equatorial ligands upon the silylation of the uranyl U–O bond.

Keywords: density functional calculations · equatorial ligands · macrocycles · silylation · uranium

Introduction

The chemistry of uranium is dominated by the dioxo or uranyl dication, $[UO_2]^{2+}$, which is found both in aqueous solutions and in the solid state. It is chemically robust[1] and shows little propensity to participate in the myriad reactions that are characteristic of its Group 6 transition-metal analogues, $[MO_2]^{2+}$.[2–6] Furthermore, this stability coupled with its mobility in the aqueous phase means that it is a problematic environmental contaminant.[7–9] A better understanding of the reduction of the mobile uranyl ion to insoluble U^{IV} phases, through the pentavalent $[UO_2]^{+}$ ion, is important in the context of environmental immobilization and the treatment of mixed waste.[10] As such, a renewed interest in the redox behavior of uranyl complexes in an anaerobic environment has been seen in recent years.[11–13]

Recently, we (Arnold and Love) showed that it is possible to address selectively the oxo groups of the uranyl (Scheme 1) by binding it within a hinged, Schiff base pyrrole macrocycle, and we were able to synthesize uranyl–transition-metal cation–cation complexes that incorporated a

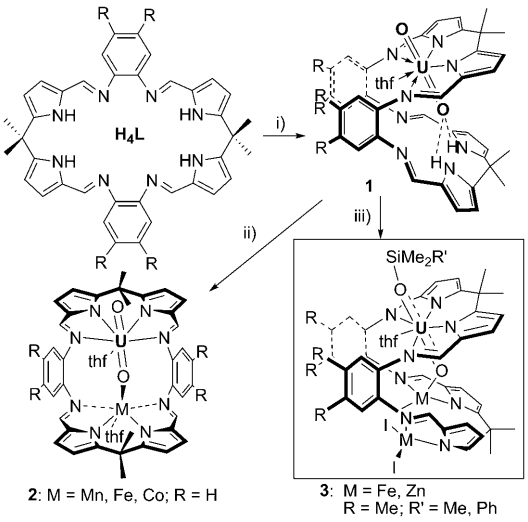

Scheme 1. Experimentally observed reactions of the macrocyclic Pacman uranyl complex **1**. i) $[UO_2(thf)_2\{N(SiMe_3)_2\}_2]$. ii) $[M\{N(SiMe_3)_2\}_2]$, thf, heat. iii) KH, MI_2, $N(SiMe_3)_3$ or $PhCH_2SiMe_3$, thf, −80 °C.

[a] A. Yahia, Prof. Dr. L. Maron
Laboratoire de Physique et Chimie des Nano-objets, INSA
Université Paul Sabatier, 135 avenue de Rangueil, 31077 Toulouse Cedex (France)
Fax: (+33) 561559697
E-mail: laurent.maron@irsamc.ups-tlse.fr

[b] A. Yahia
Institut de Chimie Séparative de Marcoule
CEA, CNRS, UM2, ENSCM
Site de Marcoule, BP 17171, 30207 Bagnols sur Cèze Cedex (France)

[c] Prof. Dr. P. L. Arnold, Dr. J. B. Love
EaStCHEM School of Chemistry, University of Edinburgh
West Mains Road, Edinburgh, EH9 3JJ (UK)

Supporting information for this article is available on the WWW under http://dx.doi.org/10.1002/chem.200902991. Cartesian coordinates of the optimized structures are included.

direct U=O–TMS bond.[14] Furthermore, the Pacman complex **1** was found to react with Si–X bonds (X = C, N) in the presence of K cations and transition-metal salts to form the reductively silylated products **3**, which represent not only rare, singly-reduced $[UO_2]^+$ species[15,16] but also the first examples of covalent bond formation of the U=O bond.[17]

In this latter reaction, we proposed that the initial KH deprotonation of **1** forms a highly oxidizing dipotassium–uranyl complex (**K_2-1**), which reacted with silyl substrates through N–Si or C–Si bond homolysis, thus forming the oxo-silylated f^1 pentavalent uranyl complex $[UO(OSiMe_3)(thf)M_2X_2(\mathbf{L})]$ (**3**) after further reaction with the transition-metal salts (Scheme 2). Presumably, the dipotassium complexes are kinetically labile, but the exchange of K^+ cations for two transition-metal M^{2+} cations affords the inert, isolable, silylated uranyl complexes.

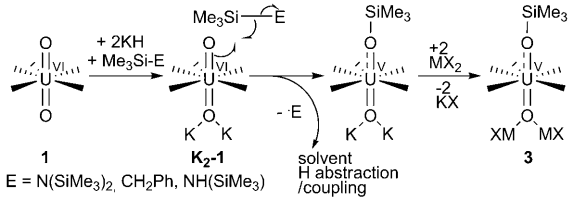

Scheme 2. Silylation reaction of the uranyl complex.

The instability of the dipotassiated uranyl adduct precluded isolation of any intermediates, but computational analysis indicated that it is a key intermediate for the silylation reaction of uranyl.[15] Indeed, it was shown that a synergic effect between dipotassiation reaction and solvent was responsible of the reductive silylation reaction of the strong U–O bond of uranyl. This analysis was carried out on a single theoretical model of the Pacman complex **1**, and we report in this paper a study of the influence of the Pacman model on the reductive silylation reaction. Moreover, the influence of the equatorial coordination sphere provided by the Pacman ligand on this reaction will be discussed by comparison with other equatorial ligands such as water.

Computational Details

Uranium was treated with a Stuttgart–Dresden pseudopotential in combination with the appropriate basis set.[18,19] In all cases, the basis set was augmented by a set of polarization functions (g for U).[20] Carbon, oxygen, nitrogen, and hydrogen atoms were described with a 6-31G(d,p) polarized double-ζ basis set.[21] Calculations were carried out at the DFT level of theory using the hybrid functional B3PW91.[22,23] Geometry optimizations were carried out without any symmetry restrictions and the nature of the extrema (minima) was verified with analytical frequency calculations. For all transition states, the intrinsic reaction coordinate was followed to verify the direct connection between the transition state and adducts. All these calculations were performed with the Gaussian 03[24] suite of programs. Gibbs free energies were obtained at 298.15 K within the harmonic approximation. The electronic density was analyzed using the natural bonding analysis (NBO) technique.[25]

Results and Discussions

Silylation of the bare uranyl ion: To understand the influence of the macrocyclic ligand, we first studied the bare uranyl ion UO_2^{2+} (uncoordinated in the equatorial plane) in the gas phase. This allows an assessment of the possible reaction pathways and a simple determination of the most favorable of these from a kinetic or thermodynamic point of view. Two different silyl substrates, Me_3SiX with X = Me and NMe_2, and three types of reaction were considered (Scheme 3.).

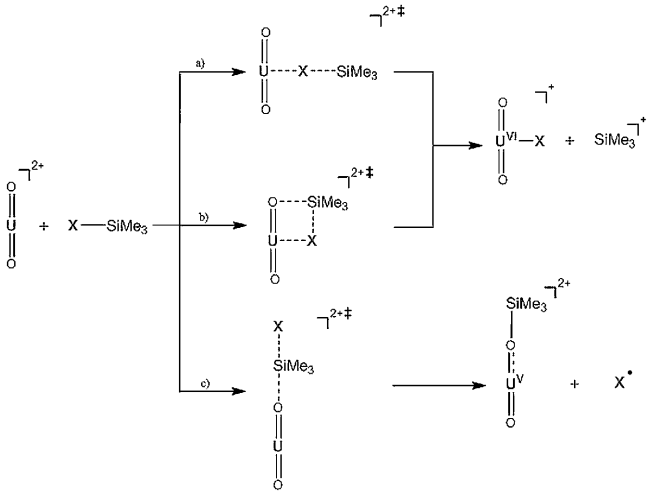

Scheme 3. The a) side-on approach, b) 2+2 reaction, and c) end-on reaction.

The side-on reaction (a) results from direct transfer of X in the equatorial plan to make a U–X bond, thus releasing a $SiMe_3$ cation. The free-energy pathway for this reaction has been computed (Figure 1).

The 2+2 reaction (b) can be better viewed as the grafting of an X substituent in the equatorial plane assisted by one of oxygen atoms of the uranyl (Figure 2).

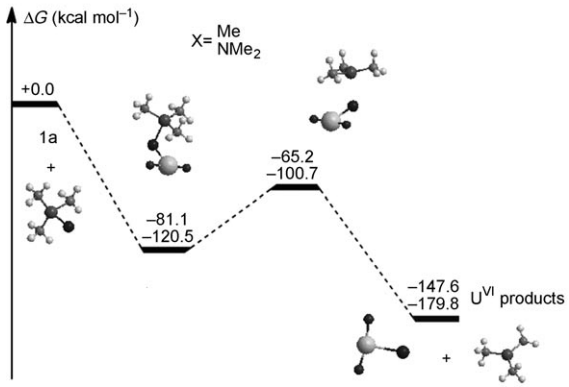

Figure 1. Free-energy profile of direct X substituent transfer in the equatorial plan.

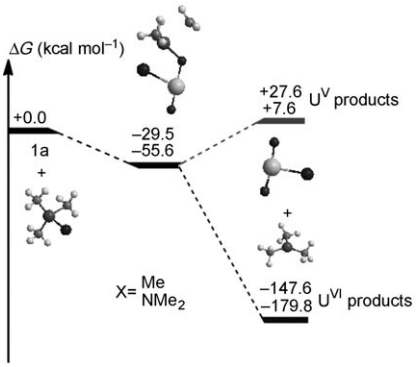

Figure 2. Free-energy profile of grafting an X substituent in the equatorial plane assisted by one uranyl oxo group.

The end-on reaction (c) is the silylation of a uranyl U−O bond with the release of an X radical (formation of silylated uranyl ion in the +V oxidation state) (Figure 3). For the silylation products, no stable structure corresponding to a silylated uranyl ion $[O{=}U{-}OSiMe_3]^+$ in a +VI oxidation state was found on the potential energy surface (PES).

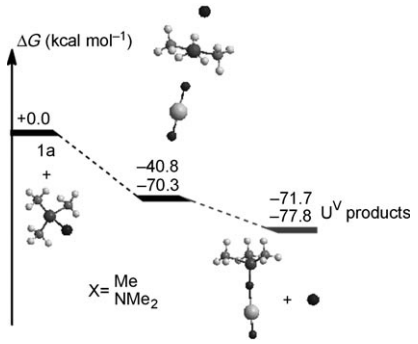

Figure 3. Free-energy profile of silylation reaction of a uranyl U−O bond.

All the reactions considered can be summarized as a competition between silicon and uranium to form an M−O bond. For all three reactions, transition states were sought for either +V and +VI oxidation states but no transition state in a +V oxidation state was located on the PES. This can be explained by the greater thermodynamic stability of the uranyl ion in the +VI oxidation state compared to the +V oxidation state. In the case of X transfer reactions (either side-on or 2+2 reactions), both are preferred kinetically and thermodynamically. More precisely, the side-on reaction is kinetically favored over the 2+2 pathway, with respective barriers of −65.2 and −29.5 kcal mol^{-1} for X=Me and −100.7 and −55.6 kcal mol^{-1} for X=NMe_2. For the side-on pathway, a very stable TMSX adduct is formed with a Gibbs free energy of coordination of −81.1 kcal mol^{-1} for X=Me and −120.5 kcal mol^{-1} for X=NMe_2, whereas for the 2+2 reaction, no stable adducts were located on the PES. Concerning the thermodynamics of the reaction, products at the +VI oxidation state are the most stable (Gibbs free energies of reactions of −147.6 kcal mol^{-1} for X=Me and −179.8 kcal mol^{-1} for X=NMe_2), whereas reactions to form U^V products are found to be endergonic (+27.6 kcal mol^{-1} for X=Me and +7.6 kcal mol^{-1} for X=NMe_2). Thus, for the X substituent transfer reaction to uranyl (side-on or 2+2), uranium does not change its oxidation state. From a comparison of the X substituent, it is clear that NMe_2 is a better leaving group than Me in both kinetic and thermodynamic terms and is due to the enhanced stability of the NMe_2 radical over the Me radical.

It is clear therefore from theoretical considerations that the side-on reaction pathway is favored in the silylation of the bare uranyl ion in the gas phase and that reductive silylation does not occur.

Influence of equatorial macrocyclic ligand binding: Since the theoretical assessment of the reductive silylation reaction was investigated previously using a single model of the macrocyclic complex,[15] the validity of the model has been evaluated using a more complete range of macrocycles that assess various aspects of the real system (Scheme 4). The retention of a macrocyclic equatorial ligand at the uranyl precludes any interaction of the substrate in the equatorial plane, so only silylation of the U−O bond may now occur.

The four models A–D contain variations of the coordination environment provided by the experimental macrocycle, with all four containing four equatorial N donors as in the real system. Model A is the simplest and is neutral; it contains two acidic NH groups. In model B, the four N donors are more accurately described as two pyrrolic N donors and two imino N donors, although unlike the real molecule, the pyrroles are still protonated. Model B also includes an ether donor, thereby mimicking the coordinated thf that occupies the fifth equatorial site in the real molecule. Model C contains the same equatorial donor set as B, but is now dianion-

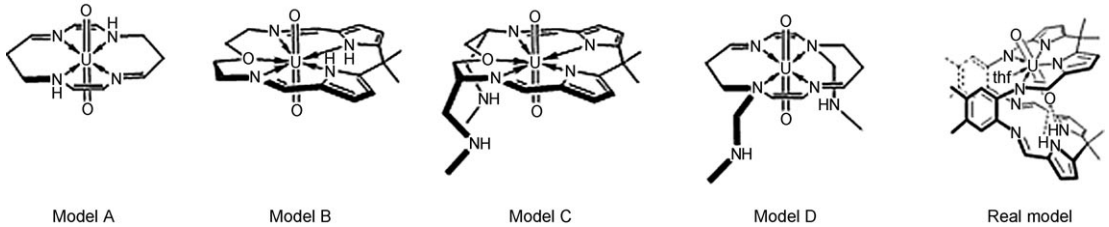

Scheme 4. ChemDraw structures of the four modeled macrocyclic complexes (A, B, C, and D) and the experimental uranyl Pacman complex (real).

ic, as in the real molecule, and the two acidic NH groups are provided by two adjacent pendant alkylamine groups. Finally, model D has the simpler N_4 donor set as in model A, but is now dianionic, and the two acidic NH groups are provided by two opposing pendant alkylamine groups.

We focused on the reaction of each U=O complex towards silylation by TMSX with X = Me and NMe_2, with the reduction of uranium to +V oxidation state and the concomitant release of an X radical (Figure 4).

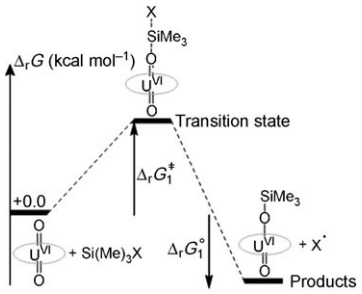

Figure 4. Free-energy profile of the silylation reaction of a U–O bond by a silane TMSX with X = Me and NMe_2, with a reduction of uranium in the +V oxidation state and the release of an X radical.

Calculations were carried out either in the gas phase or within a conductor-like polarizable continuum model (CPCM) to take into account the solvent (thf in this case). In the following, thermodynamic values will only be discussed in the gas phase, as solvent does not change the results significantly (Tables 1 and 2). Activation barriers $\Delta_r G_1^{\ddagger}$ and reaction energies $\Delta_r G_1^{\circ}$ obtained for the silylation of the U–O bond with the four models are given in Tables 1 and 2, respectively.

Table 1. The activation barrier $\Delta_r G_1^{\ddagger}$ including solvent (thf) for the silylation of the protonated models **H_2A**, **H_2B**, **H_2C**, and **H_2D** (Scheme 2) by TMSX and the release of an X radical (X = Me, NMe_2).

Model	X	$\Delta_r G_1^{\ddagger}$ [kcal mol^{-1}]	
		gas phase	with solvent model
H_2A	Me	58.4	51.0
	NMe_2	43.8	39.5
H_2B	Me	66.6	72.1
	NMe_2	48.7	46.2
H_2C	Me	87.6	80.1
	NMe_2	76.0	72.3
H_2D	Me	78.2	70.4
	NMe_2	65.3	61.8

Table 2. The free energy $\Delta_r G_1^{\circ}$ including solvent (thf) for silylation of the protonated models **H_2A**, **H_2B**, **H_2C**, and **H_2D** (Scheme 2) by TMSX and the release of an X radical (X = Me, NMe_2).

Model	X	$\Delta_r G_1^{\circ}$ [kcal mol^{-1}]	
		gas phase	with solvent model
H_2A	Me	1.7	−0.2
	NMe_2	−4.5	−9.3
H_2B	Me	−3.4	−3.1
	NMe_2	−9.4	−12.7
H_2C	Me	15.1	10.5
	NMe_2	9.0	2.7
H_2D	Me	20.4	−8.4
	NMe_2	14.3	−21.8

Kinetically, the silylation should not occur in all four cases due to the high barriers (even after the lowering of the barriers by solvent effects). Interestingly, the highest barriers are seen for the most complex models, C (87.6 kcal mol^{-1} for X = Me and 76.0 for X = NMe_2) and D (slightly lower, but the same order of magnitude). Models A and B have similar, and slightly lower barriers with a slightly more favorable reaction for the A model (58.4 kcal mol^{-1} for X = Me and 43.8 kcal mol^{-1} for X = NMe_2) than the B model (66.6 kcal mol^{-1} for X = Me and 48.7 kcal mol^{-1} for X = NMe_2). From the thermodynamic point of view ($\Delta_r G_1^{\circ}$), reactions are endergonic for C (15.1 kcal mol^{-1} for X = Me and 9.0 kcal mol^{-1} for X = NMe_2) even including solvent effects (Table 2). Reactions are endergonic for the D model in the gas phase but are exergonic including the solvent model. On the other hand, for the A and B models, reactions are exergonic except for X = Me with the A model, which is slightly endergonic in the gas phase (1.7 kcal mol^{-1}) and slightly exergonic in solution (−0.2 kcal mol^{-1}). The difference in activation barriers between the A and B models is small (roughly 5 kcal mol^{-1}), with slightly better thermodynamics for B (−3.4 kcal mol^{-1} for X = Me and −9.4 kcal mol^{-1} for X = NMe_2) than for A (1.7 kcal mol^{-1} for X = Me and −4.5 kcal mol^{-1} for X = NMe_2). Thus, the variation of the macrocycle model clearly has significant effects on the energetics of the reductive silylation reaction, and for all of these models it is clear that the silylation of the protonated uranyl macrocyclic complex is not possible, in accordance with experiments.

Deprotonation of [UO_2(mac)] prior to the silylation reaction: We proposed previously the importance of the reaction between the uranyl macrocycle complex **1** and K cations to form an intermediate that was reactive towards Si–X bond cleavage.[15,17] Thus, the silylation reactions of the U=O bond of the doubly deprotonated, K_2 complexes have been investigated (Scheme 5). Clearly, the deprotonation of models A and B occurs in the equatorial plane, whereas deprotonation of C and D occurs on the pendant chains, close to the oxo groups.

Table 3 contains the thermodynamic data for the deprotonation reactions $\Delta_r G_2^{\circ}$ obtained for the four models and the real Pacman model.

Table 3. The free energy of deprotonation reactions $\Delta_r G_2^{\circ}$ for models **H_2A**, **H_2B**, **H_2C**, **H_2D** and real macrocycle including solvent (thf).

Model	$\Delta_r G_2^{\circ}$ [kcal mol^{-1}]	
	gas phase	with solvent model
H_2A	−148.6	−100.0
H_2B	−171.0	−84.7
H_2C	−30.4	−21.6
H_2D	−89.2	−79.4
real	−95.0	−83.6

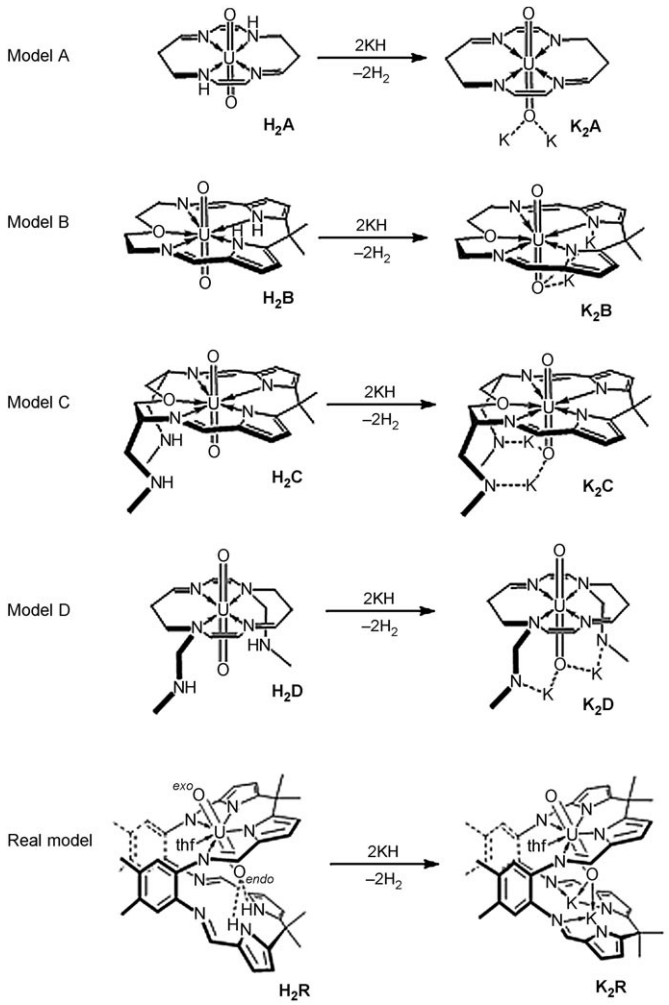

Scheme 5. Deprotonation of four model macrocycles **H_2A**, **H_2B**, **H_2C**, **H_2D** and the real macrocycle **H_2R** by potassium base KH and the formation of potassiated complexes **K_2A**, **K_2B**, **K_2C**, **K_2D**, and **K_2R**, respectively.

The thermodynamics of deprotonation ($\Delta_r G_2^\circ$) are very favorable for each case. The C model (-30.4 kcal mol^{-1} in the gas phase and -21.6 kcal mol^{-1} with CPCM) have the less favorable thermodynamics and the biggest difference with the real model (-95.0 kcal mol^{-1} in the gas phase and -83.6 kcal mol^{-1} with CPCM). Therefore model C, even though the most complete, is not the best model of the Pacman macrocyclic system. The A model has the best thermodynamics of deprotonation in the case of the CPCM (-148.6 kcal mol^{-1} in the gas phase and -100.0 kcal mol^{-1} with CPCM) but does overestimate the thermodynamics of deprotonation in comparison to the real model. The thermodynamics of deprotonation for the B model is in good agreement with the one of the real model with solvent incorporation (-171.0 kcal mol^{-1} in the gas phase and -84.7 kcal mol^{-1} with CPCM) as well as the D model (-89.2 kcal mol^{-1} in the gas phase and -79.4 kcal mol^{-1} with CPCM). Overall, for the thermodynamics of deprotonation, it is clear that the solvent correction is more important than what was found for the energies of silylation reactions. As such, an NBO analysis was carried out to understand these differences (Table 4).

For the uranium center, charge decreases during the deprotonation reaction (except for model A, in which the uranium charge increases). Potassium charges are almost the same for all models. The charges of the hydrogen atoms show that the C model contains less acidic protons (+0.24) than in the other models. The A and B models have almost the same acidity as that determined for the protons of the real model. In contrast, the protons of model D are slightly less acidic than in the A or B models due to hydrogen bonding. As expected, a correlation between the energy of deprotonation and the proton acidity is found in which an increase in proton acidity leads to a more thermodynamically favorable deprotonation. The *endo* oxygen (Figure 2) is more negatively charged than the *exo* oxygen due to their different environments, with the proximity of two hydrogen atoms (or two potassium atoms) making the *endo* oxygen more electronegative than the *exo* oxygen. During the deprotonation reaction, the charge of the *endo* oxygen increases due to the substitution of hydrogen atoms by potassium atoms, which are more electropositive. In a similar manner to the change in the *endo*-oxygen charge, the *exo*-oxygen charge increases during the deprotonation reaction, except for model B in which the charge slightly decreases. Table 5 gives U–O bond lengths for all models.

Table 5. The U–O_{endo} and U–O_{exo} distances [Å] of all protonated and potassiated complexes.

	Model A		Model B		Model C		Model D		Real model	
	H_2A	**K_2A**	**H_2B**	**K_2B**	**H_2C**	**K_2C**	**H_2D**	**K_2D**	**H_2R**	**K_2R**
U–O_{endo}	1.78	1.87	1.74	1.79	1.76	1.81	1.79	1.87	1.76	1.77
U–O_{exo}	1.75	1.75	1.74	1.74	1.76	1.76	1.79	1.79	1.74	1.74

Table 4. The NBO charges of selected groups for four models and the real model.

	Model A		Model B		Model C		Model D		Real model	
	H_2A	**K_2A**	**H_2B**	**K_2B**	**H_2C**	**K_2C**	**H_2D**	**K_2D**	**H_2R**	**K_2R**
U	2.25	2.49	3.01	2.86	3.00	2.72	2.40	2.34	3.01	2.98
O_{endo}	−0.92	−1.15	−0.9	−1.04	−0.93	−1.07	−0.94	−1.11	−0.96	−0.98
O_{exo}	−0.84	−0.87	−0.88	−0.87	−0.91	−0.93	−0.94	−0.93	−0.87	−0.9
H	0.51	–	0.49	–	0.24	–	0.40	–	0.46	–
K	–	1.00	–	0.99	–	0.95	–	0.96	–	0.97

In the protonated compounds (**H_2A**, **H_2B**, **H_2C**, **H_2D**, and **H_2R**), the U–O_{endo} and U–O_{exo} distances are almost the same, but after deprotonation, the U–O_{endo} distances increase due to the presence of potassium, which creates a strong electrostatic interaction with O_{endo}. On the other hand, the U–O_{exo} distances do not change upon deprotonation. Thus, the C model is clearly not a good model of the macrocycle in terms of reactivity, whereas A, B, and D are reasonable models. Silylation reactions from the dipotassiated complexes (**K_2A**, **K_2B**, **K_2C**, and **K_2D**) have thus been investigated (Figure 5).

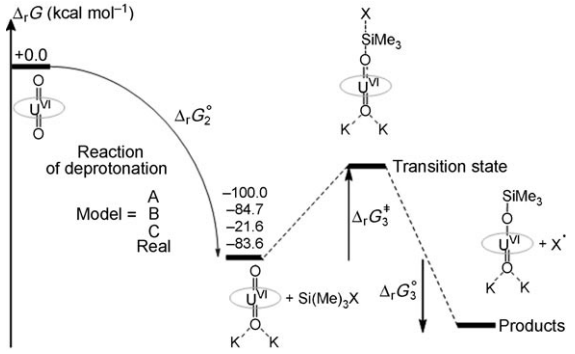

Figure 5. Free-energy profiles of silylation reactions of U–O bond by a silane TMSX with X = Me and NMe_2, with a reduction of uranium to the +V oxidation state and the release of an X radical after deprotonation.

As for the protonated compounds, the relative barriers of silylation $\Delta_rG_2^{\ddagger}$ (Tables 6 and 7) are reasonably high in the gas phase, but strongly below the entrance channel, since the deprotonation reactions are highly exergonic. Only for the C model is this barrier above the entrance channel due to lower thermodynamics of deprotonation. The latter result is not in agreement with the experiment, thereby clearly indicating once again that C is not a good model of the Pacman ligand. It is clear that the inclusion of solvent effects by means of a continuum model decreases the barriers, thus leading to an accessible reaction for the A and D models. For B, the decrease is much lower (as for C) than for A or D, and this is due to the tight constraint of the oxygen donor in the equatorial plane that makes B a poor model of the Pacman macrocycle. All reaction products of silylation are exergonic but only slightly favorable for X = Me in the A and B models. For the C model, despite exergonic products, the reaction cannot occur because the thermodynamics of deprotonation are too low. Finally, for the A and D model, reactions of silylation occur and are more favorable for Me_3SiNMe_2 than Me_3SiMe. The reactivity is controlled by the deprotonation of the N–H groups by the potassium base and the main effect of the macrocycle is to stop the reactivity of TMSX in the equatorial plane. Considering this, it is instructive to see if these reactions can occur with other ligands in the equatorial plane, for example, with five-coordinated water molecules. The high solubility of uranyl in water and the coordination flexibility compared to the macrocycle make this an interesting target.[26–40]

Table 6. The activation barrier $\Delta_rG_1^{\ddagger}$ including solvent (thf) for silylation of the models **K_2A**, **K_2B**, **K_2C**, and **K_2D** by TMSX and the release of an X radical (X = Me, NMe_2).

Model	X	$\Delta_rG_3^{\ddagger}$ [kcal mol^{-1}]	
		gas phase	with solvent model
K_2A	Me	76.3	64.7
	NMe_2	62.2	38.8
K_2B	Me	76.7	71.2
	NMe_2	61.3	53.6
K_2C	Me	78.4	74.6
	NMe_2	66.2	58.5
K_2D	Me	45.4	41.5
	NMe_2	34.3	36.5

Table 7. The free energy $\Delta_rG_3^{\circ}$ including solvent (thf) for silylation of the model **K_2A**, **K_2B**, **K_2C**, and **K_2D** by TMSX and the release of an X radical (X = Me, NMe_2).

Model	X	$\Delta_rG_3^{\circ}$ [kcal mol^{-1}]	
		gas phase	with solvent model
K_2A	Me	−0.4	−0.8
	NMe_2	−6.4	−15.8
K_2B	Me	0.2	−0.6
	NMe_2	−5.9	−9.3
K_2C	Me	−6.7	−7.1
	NMe_2	−12.8	−15.2
K_2D	Me	−14.6	−54.7
	NMe_2	−20.6	−40.1

Silylation of uranyl ion in an aqueous environment: In a manner similar to that of uranyl in a macrocyclic environment, the reductive silylation of the U–O bond of uranyl with five water molecules in the equatorial plane was investigated theoretically. Thus, we focused only on the silylation of U–O bond by the silane TMSX with X = Me and NMe_2, coupled with the reduction of uranium to +V oxidation state and the release an X radical (Figure 6).

The reactions are exergonic for the reductive silylation of U–O of the uranyl ion and the concomitant release of an X

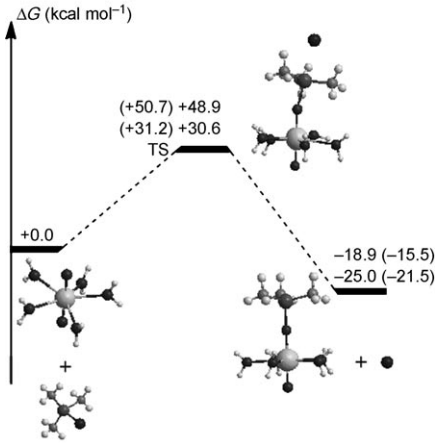

Figure 6. Free-energy profile computed and calculated for the reaction of silylation of the U–O bond of $[UO_2(H_2O)_5]$ with TMSX; the gas-phase energies are given in parentheses.

radical (-15.5 kcal mol^{-1} for X = Me and -21.5 kcal mol^{-1} for X = NMe_2). The solvent effect (water) slightly increases the thermodynamics of the reaction (-18.9 kcal mol^{-1} for X = Me and -25.0 kcal mol^{-1} for X = NMe_2). Kinetically, there is a difference between the two X substituents, as the reaction is inaccessible for X = Me (activation barrier of 50.7 kcal mol^{-1} in the gas phase and 48.9 kcal mol^{-1} with solvent effect), whereas it is accessible for X = NMe_2 (31.2 kcal mol^{-1} in the gas phase and 30.6 kcal mol^{-1} with solvent effect). As for uranyl in a macrocyclic environment above,[15] the transition states can be described as an S_N type with a cationic silyl in mid-transfer between the X radical (Me or NMe_2) and the oxo group of uranyl. Thus, the silylation of uranyl in a water environment could occur if an appropriate water-stable aminosilane could be identified. It is interesting to note that Berthet and co-workers[41] observed the formation of $UI_4(MeCN)_4$ from $UO_2I_2(thf)_3$ or $UO_2I_2(OTf)_2$ and excess Me_3SiI, although the presence of intermediates was not discussed. However, reactions were carried out in MeCN and not water. As shown for uranyl in a macrocyclic environment, deprotonation by a potassium base is an important issue. As such, the free Gibbs energies have been computed for the deprotonation of two coordinated equatorial water molecules by two equivalents of potassium base, here KH (Scheme 6).

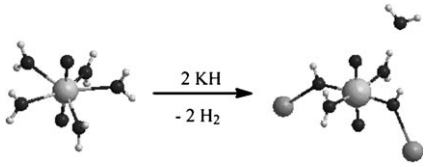

Scheme 6. Deprotonation of $[UO_2(H_2O)_5]$ by KH and formation of the cation–cation complex $[UO_2(H_2O)_2(KOH)_2]\cdot H_2O$.

This deprotonation reaction was also found to be very favorable thermodynamically (-188.6 kcal mol^{-1} in the gas phase and -71.2 kcal mol^{-1} with solvent continuum). Moreover, the loss of a water molecule from the equatorial plane is observed upon deprotonation, thereby forming a uranyl center with an unusual four-coordinate equatorial plane. The two coordinated KOH molecules form further electrostatic interactions between the two potassium cations at the same uranyl oxo atom, thus inducing considerable rigidity to this compound (Scheme 7). It is notable that both potassium cations coordinate to the same oxo ion, even in the absence of a directing macrocycle.

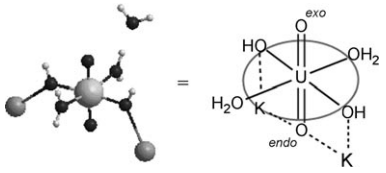

Scheme 7. Cation–cation interaction in the complex $[UO_2(H_2O)_2(KOH)_2]\cdot H_2O$.

Thus, the product of deprotonation $[UO_2(H_2O)_2(KOH)_2]\cdot H_2O$ reduces the accessibility for the silane of the equatorial plane compared with the complex $[UO_2(H_2O)_5]$ due to strong electrostatic interaction between the OH and the uranium center. The displacement of a ligand in the equatorial plane to allow the coordination of the silane is thus unlikely to occur. As for $[UO_2(H_2O)_5]$, the Gibbs free-energy profiles have been computed for the silylation of the U–O bond of $[UO_2(H_2O)_2(KOH)_2]\cdot H_2O$ with TMSX (Figure 7).

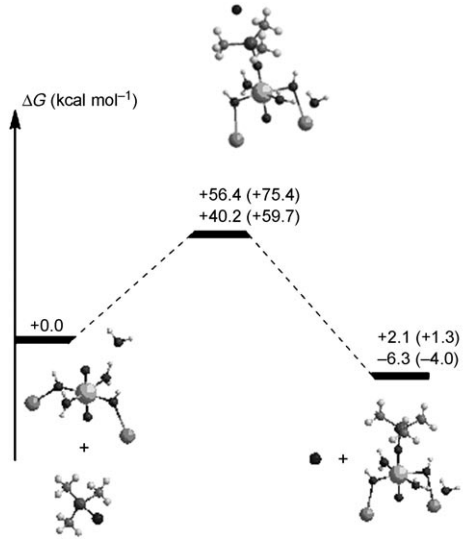

Figure 7. Free-energy profile computed and calculated for the reaction of silylation of the U–O bond of $[UO_2(H_2O)_2(KOH)_2]\cdot H_2O$ with TMSX; the gas-phase energies are given in parentheses.

The reaction of $[UO_2(H_2O)_2(KOH)_2]\cdot H_2O$ with $SiMe_4$ is slightly endergonic (1.3 kcal mol^{-1} in the gas phase and 2.1 kcal mol^{-1} with solvent effect) and the reaction is exergonic with the aminosilane (-4.0 kcal mol^{-1} in the gas phase and -6.3 kcal mol^{-1} with solvent effect). These two reactions are less favorable than the same silylation reactions starting from $[UO_2(H_2O)_5]$. Although the activation barriers are high for the two silanes Me_3SiMe and Me_3SiNMe_2, the reaction is thermodynamically favorable with the latter aminosilane. The question of the reactivity in the equatorial plane of $[UO_2(H_2O)_2(KOH)_2]\cdot H_2O$ is crucial because the reactivity in the equatorial plane is in competition with the oxo-group silylation. Because the equatorial plane of $[UO_2(H_2O)_2(KOH)_2]\cdot H_2O$ is less accessible than in $[UO_2(H_2O)_5]$, we can predict that the silylation of $[UO_2(H_2O)_2(KOH)_2]\cdot H_2O$ with the aminosilane can probably occur in a water environment.

Conclusion

We have shown that the reductive silylation of the U−O bond of uranyl with TMSX is dependent upon the accessibility of the silane substrate to the equatorial plane, and that the deprotonation of the ligand plays a crucial role for the reductive silylation of uranyl due to a very favorable thermodynamic term. This result is in agreement with the experimental observation that the reaction does not occur in the absence of a potassium base. The potassium cations do not participate in the silylation reaction pathway and instead remain coordinated to the macrocyclic ligand and the *endo* oxygen of uranyl. Moreover, in an aqueous environment, the presence of potassium cations leads to a particularly rigid but low-coordinate equatorial plane at uranyl. We are currently investigating the influence of different bases upon the mono-oxo selectivity, and the potential for this silylation chemistry to operate with the heavier actinyls, namely, neptunyl and plutonyl.

Acknowledgements

We thank the Insitut Universitaire de France, CALMIP, CCRT, and CINES for their grant of computing time; CNRS, UPS, and CEA for financial support of this work; and the EPSRC and the University of Edinburgh for funding.

[1] R. G. Denning, *J. Phys. Chem. A* **2007**, *111*, 4125–4143.
[2] W. Nam, *Acc. Chem. Res.* **2007**, *40*, 522–531.
[3] N. Jin, M. Ibrahim, T. G. Spiro, J. T. Groves, *J. Am. Chem. Soc.* **2007**, *129*, 12416–12417.
[4] F. E. Kühn, A. M. Santos, M. Abrantes, *Chem. Rev.* **2006**, *106*, 2455–2475.
[5] A. S. Larsen, K. Wang, M. A. Lockwood, G. L. Rice, T. J. Won, S. Lovell, M. Sadilek, F. Turecek, J. M. Mayer, *J. Am. Chem. Soc.* **2002**, *124*, 10112–10123.
[6] J. M. Mayer, *Acc. Chem. Res.* **1998**, *31*, 441–450.
[7] M. Amme, T. Wiss, H. Thiele, P. Boulet, H. Lang, *J. Nucl. Mater.* **2005**, *341*, 209–223.
[8] Y. Suzuki, S. D. Kelly, K. M. Kemner, J. F. Banfield, *Nature* **2002**, *419*, 134–134.
[9] D. R. Lovley, E. J. P. Phillips, Y. A. Gorby, E. R. Landa, *Nature* **1991**, *350*, 413–416.
[10] S. M. Ilton, S. C. Smith, D. Elbert, C. X. Liu, *Environ. Sci. Technol.* **2006**, *40*, 5003–5009.
[11] L. Natrajan, F. Burdet, J. Pecaut, M. Mazzanti, *J. Am. Chem. Soc.* **2006**, *128*, 7152–7153.
[12] T. W. Hayton, J. M. Boncella, B. L. Scott, E. R. Batista, P. J. Hay, *J. Am. Chem. Soc.* **2006**, *128*, 10549–10559.
[13] J. C. Berthet, G. Siffredi, P. Thuery, M. Ephritikhine, *Chem. Commun.* **2006**, 3184–3186.
[14] P. L. Arnold, D. Patel, A. J. Blake, C. Wilson, J. B. Love, *J. Am. Chem. Soc.* **2006**, *128*, 9610–9611.
[15] A. Yahia, P. L. Arnold, J. B. Love, L. Maron, *Chem. Commun.* **2009**, 2402.
[16] P. L. Arnold, J. B. Love, D. Patel, *Coord. Chem. Rev.* **2009**, *253*, 1973–1978.
[17] P. L. Arnold, D. Patel, C. Wilson, J. B. Love, *Nature* **2008**, *451*, 315.
[18] D. Andrae, U. Haussermann, M. Dolg, H. Stoll, H. Preuss, *Theor. Chim. Acta* **1990**, *77*, 123–141.
[19] A. Moritz, X. Cao, M. Dolg, *Theor. Chem. Acc.* **2007**, *118*, 845–854.
[20] A. W. Ehlers, M. Bohme, S. Dapprich, A. Gobbi, A. Hollwarth, V. Jonas, K. F. Kohler, R. Stegmann, A. Veldkamp, G. Frenking, *Chem. Phys. Lett.* **1993**, *208*, 111–114.
[21] W. J. Hehre, R. Ditchfie, J. A. Pople, *J. Chem. Phys.* **1972**, *56*, 2257.
[22] A. D. Becke, *J. Chem. Phys.* **1993**, *98*, 5648–5652.
[23] K. P. Burke, J. P. Yang, *Electronic Density Functional Theory: Recent Progress and New Directions*, Springer, Heidelberg, **1998**.
[24] Gaussian 03, Revision B.05, M. J. Frisch, G. W. Trucks, H. B. Schlegel, G. E. Scuseria, M. A. Robb, J. R. Cheeseman, J. A. Montgomery, Jr., T. Vreven, K. N. Kudin, J. C. Burant, J. M. Millam, S. S. Iyengar, J. Tomasi, V. Barone, B. Mennucci, M. Cossi, G. Scalmani, N. Rega, G. A. Petersson, H. Nakatsuji, M. Hada, M. Ehara, K. Toyota, R. Fukuda, J. Hasegawa, M. Ishida, T. Nakajima, Y. Honda, O. Kitao, H. Nakai, M. Klene, X. Li, J. E. Knox, H. P. Hratchian, J. B. Cross, V. Bakken, C. Adamo, J. Jaramillo, R. Gomperts, R. E. Stratmann, O. Yazyev, A. J. Austin, R. Cammi, C. Pomelli, J. W. Ochterski, P. Y. Ayala, K. Morokuma, G. A. Voth, P. Salvador, J. J. Dannenberg, V. G. Zakrzewski, S. Dapprich, A. D. Daniels, M. C. Strain, O. Farkas, D. K. Malick, A. D. Rabuck, K. Raghavachari, J. B. Foresman, J. V. Ortiz, Q. Cui, A. G. Baboul, S. Clifford, J. Cioslowski, B. B. Stefanov, G. Liu, A. Liashenko, P. Piskorz, I. Komaromi, R. L. Martin, D. J. Fox, T. Keith, M. A. Al-Laham, C. Y. Peng, A. Nanayakkara, M. Challacombe, P. M. W. Gill, B. Johnson, W. Chen, M. W. Wong, C. Gonzalez, J. A. Pople, Gaussian, Inc., Wallingford CT, **2004**.
[25] A. E. Reed, L. A. Curtiss, F. Weinhold, *Chem. Rev.* **1988**, *88*, 899–926.
[26] G. A. Shamov, G. Schreckenbach, R. L. Martin, P. J. Hay, *Inorg. Chem.* **2008**, *47*, 1465–1475.
[27] K. I. M. Ingram, L. J. L. Haller, N. Kaltsoyannis, *Dalton Trans.* **2006**, 2403–2414.
[28] M. Garcia-Hernández, C. Willnauer, S. Kruger, L. V. Moskaleva, N. Rosch, *Inorg. Chem.* **2006**, *45*, 1356–1366.
[29] J. L. Sonnenberg, P. J. Hay, R. L. Martin, B. E. Bursten, *Inorg. Chem.* **2005**, *44*, 2255–2262.
[30] H. P. Hratchian, J. L. Sonnenberg, P. J. Hay, R. L. Martin, B. E. Bursten, H. B. Schlegel, *J. Phys. Chem. A* **2005**, *109*, 8579–8586.
[31] D. Hagberg, G. Karlstrom, B. O. Roos, L. Gagliardi, *J. Am. Chem. Soc.* **2005**, *127*, 14250–14256.
[32] Z. J. Cao, K. Balasubramanian, *J. Chem. Phys.* **2005**, *123*, 12.
[33] N. Kaltsoyannis, *Chem. Soc. Rev.* **2003**, *32*, 9–16.
[34] V. Vallet, U. Wahlgren, B. Schimmelpfennig, Z. Szabo, I. Grenthe, *J. Am. Chem. Soc.* **2001**, *123*, 11999–12008.
[35] V. Vallet, U. Wahlgren, B. Schimmelpfennig, H. Moll, Z. Szabo, I. Grenthe, *Inorg. Chem.* **2001**, *40*, 3516–3525.
[36] V. Vallet, L. Maron, B. Schimmelpfennig, T. Leininger, C. Teichteil, O. Gropen, I. Grenthe, U. Wahlgren, *J. Phys. Chem. A* **1999**, *103*, 9285–9289.
[37] S. Spencer, L. Gagliardi, N. C. Handy, A. G. Ioannou, C. K. Skylaris, A. Willetts, A. M. Simper, *J. Phys. Chem. A* **1999**, *103*, 1831–1837.
[38] C. Clavaguéra-Sarrio, S. Hoyau, N. Ismail, C. J. Marsden, *J. Phys. Chem. A* **2003**, *107*, 4515–4525.
[39] N. Ismail, J. L. Heully, T. Saue, J. P. Daudey, C. J. Marsden, *Chem. Phys. Lett.* **1999**, *300*, 296–302.
[40] W. A. de Jong, L. Visscher, W. C. Nieuwpoort, *TEOCHEM* **1999**, *458*, 41–52.
[41] J. C. Berthet, G. Siffredi, P. Thuery, M. Ephritikhine, *Eur. J. Inorg. Chem.* **2007**, 4017–4020.

Received: October 29, 2009
Published online: March 18, 2010

